2005 7th International Conference on Information Fusion (FUSION)

Re-entry vehicle tracking observability and theoretical bound

Pierre Dodin
CEA CESTA, BP 2 33114 Le Barp, France

Pierre Minvielle
CEA CESTA, BP 2 33114 Le Barp, France

Jean-Pierre Le Cadre
IRISA/CNRS, Campus de Beaulieu, Rennes, France

Abstract – *This article deals with theoretical bounds and observability in ballistic re-entry vehicle tracking; theoretical and simulation results are presented.*

One essential characteristic of this trajectory is the deceleration of the vehicle when it reaches dense atmospheric layers. The intensity of the phenomenon is proportional to a scalar, called the ballistic coefficient. This leads to highly non-linear dynamics.

We have compared tracking data processing techniques like Extended Kalman Filter (EKF) and Particle Filter to the Posterior Cramer-Rao Bound (PCRB) in order to confirm the exactness of this very bound and to evaluate at the same time the filters' performance. The observability problem of the trajectory is mostly the observability of the ballistic coefficient during the re-entry phase. Thus we have gradually studied its observability using a simple a priori random walk model, from a constant to a complex Allen oscillatory ballistic profile for the trajectory simulation. The accuracy of the particle filter and the exactness of the bound have been confirmed.

In order to understand the important parameters of the bound, we explain the evolution of the observability during the re-entry phase using the Fisher Information Matrix, the inverse of the Cramer-Rao Bound (CRB). We give an analytical expression of the CRB versus time for simple observation cases, using Cauchy-Binet formula for matrix determinants.

1 Introduction

Anti-Ballistic defenses are confronted with the challenge of detecting, in a few seconds, swift non-cooperative targets aiming at locating them precisely and to allowing interception. With Anti-Ballistic Missile (ABM) or Anti-Tactical-Ballistic (ATBM) goals, those defenses use adapted sensors, such as the millimeter wave (MMW) radar located at Kwajalein (Marshall Islands) [1] , to track re-entry vehicles (RV) with large aerodynamics loads and a sudden deceleration, leaving a quiet exo-atmospheric phase. The motion is obviously non-linear and furthermore both the extent and the evolution of the drag are impossible to predict. They both have to be estimated dynamically and may be used to differentiate hostile re-entry bodies from benign decoys. This is a non-linear filtering problem.

Non-linear filtering can be solved by linear approximations like EKF [2] , but although its complexity is very low, one must not forget that its performance can be weakened by instabilities and divergence. Sequential Monte-Carlo methods are efficient algorithms and suitable for global non-linear filtering, albeit subject to degeneracy and being a more time consuming algorithm architecture [3]. The existence of a point of performance reference like the PCRB [4] is essential. Some authors already did the comparison within a mono-dimensional ballistic model like Farina et al. [5]. As far as we know, there is no analytical explanation for the observability evolution during the re-entry phase, where the violent speed decrease renders possible the estimation of the ballistic coefficient. The purpose of this article is the performance analysis of RV tracking with complex ballistic profile, and the explanation of the essential parameters in the system observability. The study progresses along the steps proposed in reference [3] .

We study the system's observability using the inverse of the Cramer-rao Bound, the Fisher Information Matrix, or FIM. As a matter of fact, tools like formal calculus exist for the FIM, allowing the knowledge of locally important parameters around an initial condition. We show in this article that acceleration is the essential parameters for the system observability. We also give an analytical approximation of the Cramer-Rao Bound of the ballistic coefficient.

We evaluate the performance of filtering algorithms applied to the RV tracking problem. We chose two filtering algorithms for this study: the extended Kalman filter (EKF) and the particle filter. The choice of the particle filter is justified by the high non-linearity of the problem, while the EKF is a natural point of reference and furthermore has a lower complexity.

In order to evaluate the filters' performance, we have to evaluate the best possible performance of an estimation algorithm. The *a posteriori* Cramer-Rao bound [4] gives the best possible performance. At each step of time we evaluate a recursive equation whose terms are computed as a mean over a flow of trajectories. The flow is computed over all possible trajectories with

0-7803-9286-8/05/$20.00 ©2005 IEEE

different initial conditions. The ballistic coefficient is variable, using the Allen oscillatory model which describes the oscillations of the incidence angle. The estimation is made using a random walk model. One particular difficulty was the correct dimensioning of the dynamic noise of this very random walk. We show that we can take it as the upper envelope of the derivative of the ballistic coefficient β versus time. Then we study the filters robustness versus the knowledge level of the true dynamic noise.

This article has a two part structure. In the first part we study the FIM in a two dimensional simplification of dynamics with a constant β. In the second part, we compare in a general case of dynamics and β parameter the performance of EKF and particle filter with PCRB. We give a robustness analysis of the algorithms.

2 Local study of the PCRB by the Fisher Information Matrix

In this section, we will show that the observability is proportional to the object's acceleration. We start with the description of a 2D model that will be used to find analytical bounds.

2.1 Two dimension model

2.1.1 Notations and definitions

Let A be the object cross-section, C its drag coefficient and m its mass. We note β the ballistic coefficient. The ballistic coefficient is the product $\frac{CA}{m}$ and is expressed in $m^2.kg^{-1}$. We note $g_0 = -9.8m.s^{-2}$, the gravitational acceleration. We note alt the altitude; $alt = y$ in the coordinate system of figure 1. The atmospheric density is given by:
$\rho(alt) = \rho_0 exp\{-\frac{(alt)}{c_\rho}\} kg.m^{-3}$ with $c_\rho = 7000$ and $\rho_0 = 1.2kg.m^{-3}$.

2.1.2 The two-dimensional reduction

Let us deal with a classical two-dimensional reduction of the ballistic dynamics. We have represented on figure 1 a two dimension reduction of the problem. Let γ be the constant re-entry angle, and v_x, v_y the two components of the speed. The differential equations of the reduction of dimension two are the following:

$$\dot{v}_y = g_0 + sin(\gamma)\frac{1}{2}\beta.\rho(y)v^2\,,\ \dot{v}_x = cos(\gamma)\frac{1}{2}\beta.\rho(y)v^2 \quad (1)$$

Note that if g_0 is neglected compared to dynamic pressure $\frac{1}{2}\beta\rho v^2$, as suggested in Allen's article [9], then

$$\dot{v} = \frac{1}{2}\beta\rho v^2 \quad (2)$$

2.1.3 Expression of the speed versus altitude

Allen finds the following solution of (1) in [9], by considering a constant γ angle and neglecting gravity forces compared to drag forces:

$$v(y) = v[y(t_0)]exp(-\frac{1}{2sin(\gamma)}\beta\rho_0 c_\rho e^{-\frac{y}{c_\rho}}). \quad (3)$$

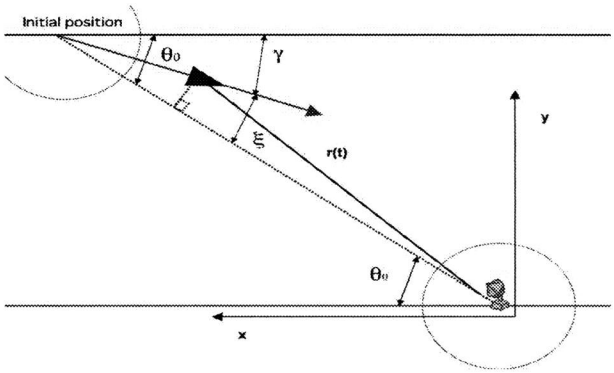

Figure 1: Two dimension reduction.

Let $r(t)$ be the range versus time. Using this expression 3 versus altitude, it is possible to obtain an exact formula versus time, e.g. $v[y(t)]$ by substituting

$$y(t) = sin(\theta_0)r(t_0) - \int_{t_0}^{t} v[y(\tau)]sin(\gamma)d\tau \quad (4)$$

in equation (3). Then $\int_{t_0}^{t} v[y(\tau)]d\tau$ is a solution of a differential equation. It is also possible to obtain - close to the initial condition - an approximation using the Taylor development of altitude as a function of time given in equation (5),

$$y(t) \approx sin(\theta_0)r(t_0) - sin(\gamma)(t - t_0)v[y(t_0)]) \quad (5)$$

2.1.4 Expression of range

In the system we have two angles, γ (the re-entry angle) and ξ (the angle between the re-entry path and the initial line of sight $\theta(0)$.) We want to evaluate the FIM for a radar observing range information and estimating r, v, β (It is possible to obtain the FIM if the radar estimates also θ, but here we suppose that θ, γ are estimated separately using bearing information).
Let us note $v[y(t)]$ the speed along the re-entry axis, and $\zeta = \pi - \xi$.
$v[y(t)]$ is decomposed into two parts: The projection along the initial line of sight and the angular or orthogonal part:

$$v_r(t) = v[y(t)]\,cos(\zeta) \quad v_a(t) = v[y(t)]\,sin(\zeta) \quad (6)$$

ζ is used to have a negative cosinus for the radial part of the speed vector.
We note $r_r(t)$ the projection of the radius along the initial line of sight, $r_a(t)$ its orthogonal part.
We suppose $r_r(t) >> r_a(t)$. If we use the relation $\sqrt{A^2 + B^2} \approx A + \frac{1}{2}\frac{B^2}{A}$, valid for real numbers such as $A >> B$, the range versus time $r(t) = \sqrt{r_r(t)^2 + r_a(t)^2}$ is given by:

$$\begin{aligned} r(t) &= \left(\left(r(t_0) + \int_{t_0}^{t} v_r d\tau\right)^2 + \left(\int_{t_0}^{t} v_a d\tau\right)^2\right)^{1/2} \\ &\approx r(t_0) + \int_{t_0}^{t} v_r d\tau + (1/2)\frac{\left(\int_{t_0}^{t} v_a d\tau\right)^2}{\left(r(t_0) + \int_{t_0}^{t} v_r d\tau\right)} \end{aligned}$$

2.2 FIM determinant calculation

Let us suppose a range-only observation function.

2.2.1 Definition of the FIM

Let $\mathbf{M}$ be the observation function gradient along the trajectory:

$$\mathbf{M}_t \equiv \left(\frac{\partial r(t)}{\partial r(t_0)}, \frac{\partial r(t)}{\partial v[y(t_0)]}, \frac{\partial r(t)}{\partial \beta}\right)' \quad (7)$$

and let $\mathbf{N}_t = \frac{1}{\sigma_r}\mathbf{M}_t$, with σ_r the range measurement standard deviation. In a range-only measurement system, the Fisher Information Matrix (FIM) is:

$$\begin{aligned}\mathbf{FIM}_{(t_0,t_k)} &= \sum_{s=t_0}^{s=t_k} \mathbf{M}_s \frac{1}{\sigma_r^2}\mathbf{M}_s' = \sum_{s=t_0}^{s=t_k} \mathbf{N}_s\mathbf{N}_s' \\ &= \mathbf{Z}\mathbf{Z}' \end{aligned} \quad (8)$$

with $\mathbf{Z} = [\mathbf{N}_{t_0}|\mathbf{N}_{t_1}|\cdots|\mathbf{N}_{t_k}]$ the matrix whose each column is the vector $\mathbf{N}_t$ from $t = t_0$ to $t = t_k$.

2.2.2 The Cauchy-Binet formula

If we want to compute the determinant $det(\mathbf{FIM}_{(t_0,t_k)}) = det(\mathbf{Z}\mathbf{Z}')$, we have the following exact formula (see [10]):

$$det(\mathbf{FIM}_{(t_0,t_k)}) = \sum_{0\le p\le q\le r\le k} det(\mathbf{N}_{t_p}, \mathbf{N}_{t_q}, \mathbf{N}_{t_r})^2$$

2.2.3 Exterior Calculus and consequences

Let us define the 3×3 square matrix

$$\mathbf{\Omega}(t) \equiv [\mathbf{M}, \frac{d\mathbf{M}}{dt}, \frac{d^2\mathbf{M}}{dt^2}](t) = [\mathbf{M}_t, \mathbf{M}_t^{(1)}, \mathbf{M}_t^{(2)}] \quad (9)$$

Expansion of the FIM around t_0.

Let $P(a,b,c)$ be:
$P(a,b,c) = \frac{bc^2}{2} + \frac{ab^2}{2} + \frac{a^2c}{2} - \frac{b^2c}{2} - \frac{ac^2}{2} - \frac{a^2b}{2}$.
Let us note $\widetilde{t_i} = t_i - t_0$. Let us suppose valid the Taylor expansion (see [10]):

$$\mathbf{M}_{t_i} = \mathbf{M}_{t_0} + \widetilde{t_i}\mathbf{M}_{t_0}^{(1)} + \frac{\widetilde{t_i}^2}{2}.\mathbf{M}_{t_0}^{(2)} \quad (10)$$

For $(x,y,z) \in \mathbf{R^3}$, let $\omega(x,y,z) = x \wedge y \wedge z$ be a multilinear antisymmetric 3-form, an element of $\Lambda^3(\mathbf{R^3})$. Then

$$det(\mathbf{M}_{t_p}, \mathbf{M}_{t_q}, \mathbf{M}_{t_r}) = P(\widetilde{t_p}, \widetilde{t_q}, \widetilde{t_r}).det(\mathbf{\Omega}(t_0)).$$

Indeed, we have

$$det(\mathbf{M}_{t_p}, \mathbf{M}_{t_q}, \mathbf{M}_{t_r}) = \mathbf{M}_{t_p} \wedge \mathbf{M}_{t_q} \wedge \mathbf{M}_{t_r}.$$

Let us note $\widetilde{t_i} = t_i - t_0$. By equation 10 we obtain:

$$\begin{aligned}&\mathbf{M}_{t_p} \wedge \mathbf{M}_{t_q} \wedge \mathbf{M}_{t_r} \\ &= \frac{\widetilde{t_q}\widetilde{t_r}^2}{2}\mathbf{M}_{t_0} \wedge \mathbf{M}_{t_0}^{(1)} \wedge \mathbf{M}_{t_0}^{(2)} + \frac{\widetilde{t_q}^2\widetilde{t_r}}{2}\mathbf{M}_{t_0} \wedge \mathbf{M}_{t_0}^{(2)} \wedge \mathbf{M}_{t_0}^{(1)} \\ &+ \frac{\widetilde{t_p}\widetilde{t_r}^2}{2}\mathbf{M}_{t_0}^{(1)} \wedge \mathbf{M}_{t_0} \wedge \mathbf{M}_{t_0}^{(2)} + \frac{\widetilde{t_p}\widetilde{t_q}^2}{2}\mathbf{M}_{t_0}^{(1)} \wedge \mathbf{M}_{t_0}^{(2)} \wedge \mathbf{M}_{t_0} \\ &+ \frac{\widetilde{t_p}^2\widetilde{t_r}}{2}\mathbf{M}_{t_0}^{(2)} \wedge \mathbf{M}_{t_0} \wedge \mathbf{M}_{t_0}^{(1)} + \frac{\widetilde{t_p}^2\widetilde{t_q}}{2}\mathbf{M}_{t_0}^{(2)} \wedge \mathbf{M}_{t_0}^{(1)} \wedge \mathbf{M}_{t_0} \\ &= P(\widetilde{t_p}, \widetilde{t_q}, \widetilde{t_r})\mathbf{M}_{t_0} \wedge \mathbf{M}_{t_0}^{(1)} \wedge \mathbf{M}_{t_0}^{(2)}.\end{aligned}$$

The consequence is the simple expression of the FIM determinant:

$$\begin{aligned}&det(\mathbf{FIM}_{(t_0,t_k)}) = \frac{1}{\sigma_r^6} \sum_{0\le p\le q\le r\le k} det(\mathbf{M}_{t_p}, \mathbf{M}_{t_q}, \mathbf{M}_{t_r})^2 \\ &= R(k)det(\mathbf{\Omega}(t_0)). \text{ with} \\ &R(k) = \sum_{p\le q\le r\le k} P(t_p - t_0, t_q - t_0, t_r - t_0)^2\end{aligned}$$

Expansion of the FIM around successive step of time.

The highly non-linear dynamics are leading to a growing error in the Taylor approximation of formula 10, if all terms are computed based on the matrix $det(\mathbf{M}, \frac{d\mathbf{M}}{dt}, \frac{d^2\mathbf{M}}{dt^2})(t_0)$, at the initial instant t_0.
Then we can decompose the determinant to compute it based on Taylor expansions (10) evaluated around different intants $t_0, \cdots, t_k$. The decomposition is as follows:

$$\begin{aligned}&det(\mathbf{FIM}_{(t_0,t_k)}) = \frac{1}{\sigma_r^6} \sum_{0\le p\le q\le r\le k} det(\mathbf{M}_{t_p}, \mathbf{M}_{t_q}, \mathbf{M}_{t_r})^2 \\ &= \frac{1}{\sigma_r^6} \sum_{0\le q\le k} \sum_{p\le q\le r\le k} det(\mathbf{M}_{t_q+(t_p-t_q)}, \mathbf{M}_{t_q}, \mathbf{M}_{t_q+(t_r-t_q)})^2 \\ &= \frac{1}{\sigma_r^6} \sum_{0\le q\le k} S(q).det(\mathbf{\Omega}(t_q))^2 \text{ with} \\ &S(q) = \sum_{p\le q\le r\le k} P(t_p - t_q, 0, t_r - t_q)^2\end{aligned}$$

2.2.4 Computation of the matrix $\mathbf{\Omega}$

To compute the matrix $\mathbf{\Omega}$ we will need some approximations. Using the system of exact equations (3) and (4), we show in the lemma 1, given in appendix, the following approximations of equations (11,12,13,14,15).

$$\begin{aligned}\frac{\partial v[y(t)]}{\partial r(t_0)} &\approx \epsilon(t)\frac{sin(\theta_0)}{sin(\gamma)} \approx 0 && (11)\\ \frac{\partial v[y(t)]}{\partial v[y(t_0)]} &\approx \frac{v[y(t)]}{v[y(t_0)]} && (12)\\ \frac{d}{dt}\frac{\partial v[y](t)}{\partial r(t_0)} &\approx \dot{\epsilon}(t)\frac{sin(\theta_0)}{sin(\gamma)} \approx 0 && (13)\\ \frac{d}{dt}\frac{\partial v[y](t)}{\partial v[y(t_0)]} &\approx \epsilon(t) \approx 0 && (14)\\ \frac{d}{dt}\frac{\partial v[y](t)}{\partial \beta(t_0)} &\approx \frac{1}{2}\rho(t)v^2 && (15)\\ \text{with } \epsilon(t) &\equiv \frac{1}{2}\beta.\rho(t)v[y(t)] && (16)\end{aligned}$$

These approximations are valid if $\epsilon(t)$ is small w.r.t. 1, a reasonable hypothesis. Indeed in our application $v \approx c.10^3 m.s^{-1}, \beta \approx 1.10^{-4} m^2.kg^{-1}$, and $\epsilon(t) \approx \frac{c\rho(t)}{20}$. We also suppose that γ is "big enough" too avoid singular values. To have an idea of ρ values, $\rho = 1.10^{-4}$ at 65 km of altitude, $\rho = 2.10^{-3}$ at 45 km of altitude and $\rho = 1.2$ at altitude zero. We have the following property:

Property 1 *Let us suppose valid the approximations of equation (11,12,13,14,15), and* $r_r(t) >> r_a(t)$. *Then* $\mathbf{\Omega}(t)$ *is triangular and*
1) $det(\mathbf{\Omega}(t)) \approx \mathbf{\Omega}_{[1,1]}(t)\,\mathbf{\Omega}_{[2,2]}(t)\,\mathbf{\Omega}_{[3,3]}(t)$.
2) If the dynamic has no orthogonal part (ξ=0),

$$det(\mathbf{\Omega}(t)) \approx \frac{v_r}{v[y(t_0)]}\frac{1}{2}\rho(t)v^2 = \frac{v_r(t)}{v[y(t_0)]}\frac{\dot{v}(t)}{\beta}$$

Proof: Let us set $X = r(t_0) + \int_{t_0}^{t} v_r d\tau, Y = \int_{t_0}^{t} v_a d\tau$.
1) $\mathbf{\Omega}_{[1,2]}$ By lemma 2 equation (34) and approximations of equation (11), we have

$$\mathbf{\Omega}_{[1,2]} \equiv \frac{d}{dt}\frac{\partial r}{\partial r(t_0)} \approx \frac{\partial Y}{\partial r(t_0)}\frac{v_a}{X}$$

But $\frac{\partial Y}{\partial r(t_0)}(t) = \int_{t_0}^{t}\frac{\partial v_a}{\partial r(t_0)}(\tau)d\tau = \int_{t_0}^{t}\epsilon(\tau)d\tau$ and $\frac{\partial Y}{\partial r(t_0)}\frac{v_a}{X} \approx 0$ hence $\mathbf{\Omega}_{[1,2]} \approx 0$.
2) $\mathbf{\Omega}_{[1,3]}$ By the lemma 2 equation (35) and approximations of equation (13), we have

$$\mathbf{\Omega}_{[1,3]} \equiv \frac{d^2}{dt^2}\frac{\partial r}{\partial r(t_0)} \approx \frac{\partial Y}{\partial r(t_0)}\frac{\dot{v}_a}{X}$$

hence $\mathbf{\Omega}_{[1,3]} \approx 0$.
3) $\mathbf{\Omega}_{[2,3]}$ By the lemma 2 equation (35) and approximations of equation (14), we have

$$\mathbf{\Omega}_{[2,3]} \equiv \frac{d^2}{dt^2}\frac{\partial r}{\partial v[y(t_0)]} \approx \frac{\partial Y}{\partial v[y(t_0)]}\frac{\dot{v}_a}{X}$$

But $\frac{\partial Y}{\partial v[y(t_0)]}(t) = \int_{t_0}^{t}\frac{\partial v_a}{\partial v[y(t_0)]}(\tau)d\tau \approx sin(\zeta)\int_{t_0}^{t}\frac{v(\tau)}{v(t_0)}d\tau \leq sin(\zeta).(t-t_0)$ because $v(t_0) \geq v(t)$ and $\frac{\partial Y}{\partial v[y(t_0)]}\frac{\dot{v}_a}{X} \approx 0$ hence $\mathbf{\Omega}_{[2,3]} \approx 0$.
4) Let us now compute the diagonal terms. By the lemma 2 equation (33) and approximation of equation (11) we obtain

$$\begin{aligned}\mathbf{\Omega}_{[1,1]} &= \frac{\partial r}{\partial r(t_0)} \approx 1 + \int_{t_0}^{t}\epsilon(\tau)cos(\zeta)d\tau \\ &+ \int_{t_0}^{t}\epsilon(\tau)sin(\zeta)\frac{Y}{X}d\tau. \qquad (17)\end{aligned}$$

By the lemma 2 equation (34) and approximation of equation (12) we obtain

$$\mathbf{\Omega}_{[2,2]} = \frac{d}{dt}\frac{\partial r}{\partial v[y(t_0)]} \approx \frac{v_r}{v[y(t_0)]} + \frac{Y}{X}\frac{v_a}{v[y(t_0)]} \qquad (18)$$

By the lemma 2 equation (35) and approximation of equation (15) we obtain

$$\begin{aligned}\mathbf{\Omega}_{[3,3]} &= \frac{d^2}{dt^2}\frac{\partial r}{\partial \beta} \approx \frac{\partial \dot{v}_r}{\partial \beta} + \frac{Y}{X}\frac{\partial \dot{v}_a}{\partial \beta} + 2\frac{\partial v_a}{\partial \beta}\frac{v_a}{X} + \frac{\partial Y}{\partial \beta}\frac{\dot{v}_a}{X} \\ &\approx \frac{\dot{v}_r}{\beta} + (\theta-\theta_0)\frac{\dot{v}_a}{\beta} + 2\frac{[v_a(t)-v_a(t_0)]}{\beta}\dot{\theta} \\ &+ \frac{[Y(t)-Y(t_0)]-(t-t_0)v_a(t_0)}{\beta}\ddot{\theta} \qquad (19)\end{aligned}$$

The first part of the term is the division of the acceleration by β, and the second part can be understood if we remark that $\frac{Y}{X} \approx \theta, \frac{v_a}{X} \approx \dot{\theta}, \frac{\dot{v}_a}{X} \approx \ddot{\theta}$ (because X is supposed much bigger than Y). Hence the information about non-radial component is proportional to the variation of θ, multiplied by the first $(\frac{\partial v_a}{\partial \beta(0)})$ and second $(\frac{\partial Y}{\partial \beta(0)})$ integral of $\frac{\dot{v}_a}{\beta}$.

2.3 Computation of the CRB of coefficient β

Let us compute the CRB for the coefficient β in range only case. With a dynamic with no orthogonal part ($\xi = 0$). Other cases can be derived easily.
We suppose the time divided into periods $[t_0, t_2, \cdots, t_k]$. We suppose the existence of a first period t_{-1}. The matrix $\mathbf{F0} \equiv \mathbf{FIM}_{(t_{-1},t_{-1})}$ represents *a priori* information. Let us note $(\sigma_r^*, \sigma_v^*, \sigma_\beta)$ the *a priori* errors on r, v, β. We can suppose the matrix $\mathbf{F0}$ diagonal with $\mathbf{F0}_{[1,1]} \equiv \frac{1}{(\sigma_r^*)^2}, \mathbf{F0}_{[2,2]} \equiv \frac{1}{(\sigma_v^*)^2}, \mathbf{F0}_{[3,3]} \equiv \frac{1}{(\sigma_\beta)^2}$
The FIM expression is then:

$$\mathbf{FIM}_{(t_{-1},t_k)} = \mathbf{F0} + \mathbf{FIM}_{(t_0,t_k)}.$$

The $\mathbf{CRB}_\beta$ of the coefficient β is the term (3,3) in the inverse matrix $\mathbf{FIM}_{(t_{-1},t_k)}$. Let $\mathbf{A}$ be the (2,2) matrix extracted from $\mathbf{FIM}_{(t_{-1},t_k)}$, excluding the last column and last line. Using the well known property of inverse matrix we obtain:

$$\mathbf{CRB}_\beta = \frac{1}{det(\mathbf{FIM}_{(t_{-1},t_k)})}.det(\mathbf{A}).$$

The matrix A can easily be obtained from the definition of the FIM (equation (8)) and from the value of $f_i \equiv \frac{1}{\sigma_r^2}\frac{\partial r(t_i)}{\partial r(t_0)} \approx \frac{1}{\sigma_r^2}$ and $g_i \equiv \frac{1}{\sigma_r^2}\frac{\partial r(t_i)}{\partial v[y(t_0)]} \approx \frac{1}{\sigma_r^2}\int_{t_0}^{t_i}\frac{v_r(s)}{v[y(t_0)]}ds = \frac{X(t_i)-X(t_0)}{\sigma_r^2 v[y(t_0)]}$ from equation (17) and (18). Using the determinant multi-linearity we obtain:

$$det(\mathbf{A}) = det\begin{pmatrix} \frac{1}{(\sigma_r^*)^2} + \sum_{s=0}^{k} f_s^2 & \sum_{r=t_0}^{t_k} f_s g_s \\ \sum_{s=0}^{k} f_s g_s & \frac{1}{(\sigma_v^*)^2} + \sum_{s=0}^{k} g_s^2 \end{pmatrix}$$

$$= \frac{1}{(\sigma_r^*\sigma_v^*)^2} + \sum_{0\leq p\leq q\leq k}(f_p g_q - f_q g_p)^2 + \sum_{s=0}^{k}(\frac{g_s^2}{(\sigma_r^*)^2} + \frac{f_s^2}{(\sigma_v^*)^2})$$

To finish the computation, we just divide the two determinants, and take into account the initial knowledge. And because
$det(\mathbf{FIM}_{(t_{-1},t_k)}^{1/3}) \geq (det(\mathbf{F0})^{1/3} + det(\mathbf{FIM}_{(t_0,t_k)})^{1/3})^3$
We obtain:

$$|\mathbf{CRB}_\beta(t_k)| \leq \frac{det(\mathbf{A})}{(\frac{1}{(\sigma_v^*\sigma_r^*\sigma_\beta)^{2/3}} + (\frac{1}{\sigma_r^6}\sum_{0\leq q\leq k} S(q).(\frac{v_r(t_q)}{v[y(t_0)]}\frac{1}{2}\rho(t_q)v^2)^2)^{1/3})^3}$$

This function obtained has initial value σ_β and is brutally decreasing as soon as the quotient $\frac{\dot{v}}{\beta} = \frac{1}{2}\rho(t).v^2$ becomes impossible to neglect. This happens around an altitude of 65 km, giving $\rho(t).v^2 = c.100$ if $v = c.10^3 m.s^{-1}$ We give an example in figure 2, where altitude 65 km is related to the period 9 of the graph. We trace in blue the function $\sqrt{\mathbf{CRB}_\beta}$ and in red the real CRB.

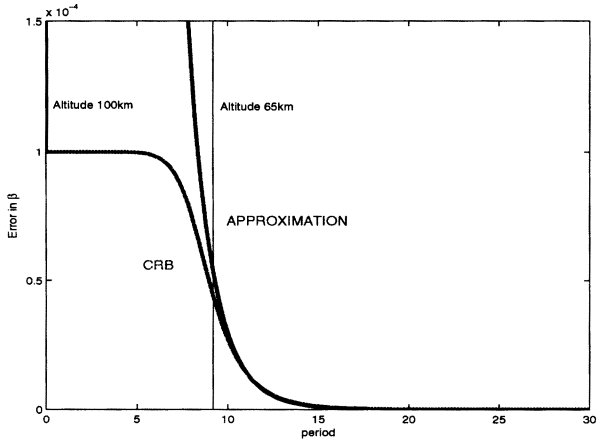

Figure 2: The error graph $\sqrt{\mathbf{CRB}(\beta)}$ in function of the periods

3 PCRB of the general model

In RV tracking, the aim is to be able to estimate the object's position, speed and ballistic coefficient, using on one hand *a priori* dynamic and measurement model, on the other hand radar observations.
Finding a good simulation model reveals high complexity, for two reasons: the first reason is the very high level of dynamic non-linearity. The second reason is the existence of non-deterministic parameters like the ballistic coefficient, which is the product of the object cross-section by the drag divided by the mass. The evolution versus time of the drag coefficient depends on the incidence angle. Allen [6] proved the very high variability of the incidence angle for a RV, inducing the same level of variability for the ballistic coefficient. In the simulations, we will use either a constant ballistic profile as a simplification and a reference, or a complex Allen profile.
Finding a good *a priori* dynamical model is a complex task too. Like in [3] and [5] , it is possible to suppose only a random walk model for the ballistic coefficient. First we describe the simulation models in subsection 3.1.1, then we give the *a priori* model used in the tracking and PCRB algorithms in subsection 3.1.2.

3.1 Modeling

3.1.1 Dynamic model for trajectory simulations

We suppose now an earth-centered coordinate system (ECF, see [3]) . We note R_e the earth radius. We note alt the altitude; $alt = \sqrt{x^2+y^2+z^2} - R_e$ in ECF. We note Ω the earth rotation speed, expressed in $rad.s^{-1}$. We describe the deterministic dynamical models that we use to generate the trajectories of our simulations.

The deterministic trajectory of the object with a constant β follows the differential equations given by:

Dynamic $\dot{\mathbf{X}} = V(\mathbf{X})$, $\mathbf{X} = (x, y, z, v_x, v_y, v_z, \beta)'$:

$$\begin{bmatrix} \dot{x} \\ \dot{y} \\ \dot{z} \\ \dot{v_x} \\ \dot{v_y} \\ \dot{v_z} \\ \dot{\beta} \end{bmatrix} = \begin{bmatrix} v_x \\ v_y \\ v_z \\ G_x + \Omega^2 x + 2\Omega v_y - q\beta\frac{v_x}{\mathbf{v}} \\ G_y + \Omega^2 y - 2\Omega v_x - q\beta\frac{v_y}{\mathbf{v}} \\ G_z - q\beta\frac{v_z}{\mathbf{v}} \\ 0 \end{bmatrix} \quad (20)$$

$$\text{with } q = \frac{1}{2}\rho\|\mathbf{v}\|^2,\ \rho = \rho_0 exp\{-\frac{(alt)}{c_\rho}\} \text{ and gravity}$$

$$\text{field } G_{x_i} = x_i \frac{g_0 R_e R_e}{r^3}\ x_i = x, y, z$$

The coefficient $q = \frac{1}{2}\rho\|v\|^2$ is the dynamic pressure. Note that this model restricted to the equator, with $z = v_z = 0$ is of dimension two, hence the analysis of the previous section is valid. The discretization of this model is used in the PCRB algorithm, in the particle filter and in the EKF. We give this discretization in subsection 3.1.3.

In our study the ballistic coefficient depends on altitude. To equation (20), we thus put out $\dot{\beta} = 0$, and we use the $\beta(alt)$ profile versus altitude, given on figure 3 (details are given in [6]).

3.1.2 *A priori* dynamic model

In this section, we describe the dynamic model the estimator supposes. It is called an *a priori* model. In the model, the differences observed between measurements and the *a priori* model will be modeled by an additive dynamic noise on the coefficient β after discretization. If the continuous *a priori* model of β is $\dot{\beta} = 0$, its discretization gives, by adding an additive dynamic noise ν_β : $\beta(k+1) = \beta(k) + \nu_\beta(k)$.(The noise sequence $\nu_\beta(k)$ is supposed white and gaussian). This is a random walk model.

3.1.3 Dynamical model discretization

Let Δt be the step of the filtering algorithm.
We suppose discrete time instants, indexed by k, $(t_1, t_2, \cdots, t_k)$, such as $t_{k+1} = t_k + \Delta t$.
We will use the notation $x(k) = x(t_k), x(k+1) = x(t_k + \Delta t)$ for each state coordinate x.
The most direct discretization consists in a finite difference. If we write equation (20) as:
$\dot{\mathbf{X}} = \mathbf{V}(\mathbf{X})$ we obtain:

$$\mathbf{X}(t_k + \Delta t) = \mathbf{f}(\mathbf{X}(t_k)) \equiv \mathbf{X}(t_k) + \Delta t \mathbf{V}(\mathbf{X}(t_k))$$

For our estimation algorithms, we should add a dynamic noise. Thus we write a model with noise: $\mathbf{X}(t_k + \Delta t) = \mathbf{f}(\mathbf{X}(t_k)) + \nu(t_k)\ \nu(t_k) \sim \mathbf{Q}(t_k)$ We may write the model more simply, as follows:

$$\mathbf{X}(k+1) = \mathbf{f}(\mathbf{X}(k)) + \nu(k)\ \nu(k) \sim \mathbf{Q}(k)$$

$\mathbf{Q}(k)$ is the Gaussian dynamic noise covariance matrix.

3.1.4 Measurement models

Our radar model gives measurement in range d and angular measurement - the direct cosines (α, μ, η).
Using a coordinate transformation matrix $\mathbf{M_r}$, and with a radar located on earth with coordinates (x_r, y_r, z_r), we obtain the measurements vector $\mathbf{h(X)}$:

$$\begin{aligned} \mathbf{h(X)} &= (\mu,\ \eta,\ d)' \text{ with} \\ (\alpha,\ \mu,\ \eta)' &\equiv \frac{\mathbf{M_r}}{d}.(x(k)-x_r,\ y(k)-y_r,\ z(k)-z_r)' \\ &+ (\nu_\mu(k),\ \nu_\eta(k),\ \nu_d(k))' \end{aligned}$$

The measurement noise sequence $(\nu_\mu(k), \nu_\eta(k), \nu_d(k))'$ is supposed white and gaussian and has a standard deviation for each coordinate, such as $\sigma_\mu = \sigma_\eta = 3.5\,10^{-5}$, and $\sigma_d = 1$ m, like in [3]. The radar is placed on the equator at longitude zero.

3.2 Comparison between PCRB and filters, Robustness of the filters

We will study the performance of the EKF and of particle filters. These filters are compared with an algorithm establishing the maximum performance that can be reached by any filter. This is equivalent to find the lower bound of the empirical state covariance. The lower bound is called the *a posteriori* Cramer Rao Bound [4].

In this section, we compare the PCRB with particle filter and EKF. The particle filter is the same as the filter described in [7] and [3], with 10000 particles. We start with a constant β, then we use a variable β, following the Allen oscillatory model. The initial vector (x, y, z, v_x, v_y, v_z) is set to $(6485921.9; -256897.4; 1.2\times 10^5; -2627.6; 6271.8; 0)$. The initial altitude is $120km$, the period is $dt = 0.5s$, and the intense braking phase starts at $60km$, i.e. 45.

3.2.1 Comparisons between PCRB and filters

During the experiences realized on PCRB and EKF filters, we observed the necessity of a correct dimensioning on the coefficient β. Let us show how it can be done.
The β dynamic can be described by

$$\beta(t_k + \Delta t) = \beta(k) + \nu(k)\,,\ \nu(k) \sim N(0, \sigma_\nu^2)$$

The finite variation theorem gives:

$$|\beta(t_k + \Delta t) - \beta(k)| \leq \max_{\epsilon\in[t_k, t_k+\Delta t]} \frac{d\beta}{dt}(\epsilon)\Delta t \quad (21)$$

Hence

$$\sigma_\nu^2 = E|\beta(t_k + \Delta t) - \beta(k)|^2 \leq \{\max_{\epsilon\in[t_k, t_k+\Delta t]} \frac{d\beta}{dt}(\epsilon)\Delta t\}^2$$

Let us note r the altitude, and ϵ^* the value of ϵ which realizes the maximum of (21). It appears clearly that we can choose: $\sigma_\nu = \frac{d\beta}{dt}(\epsilon^*)\Delta t$ Because β is expressed with altitude, we will take σ_ν, helped by the chain rule, equals to : $\sigma_\nu \simeq \frac{dr}{dt}(\epsilon^*)\widetilde{\frac{d\beta}{dr}}\Delta t$ If we suppose known $\widetilde{\frac{d\beta}{dr}} \simeq \frac{d\beta}{dr}$

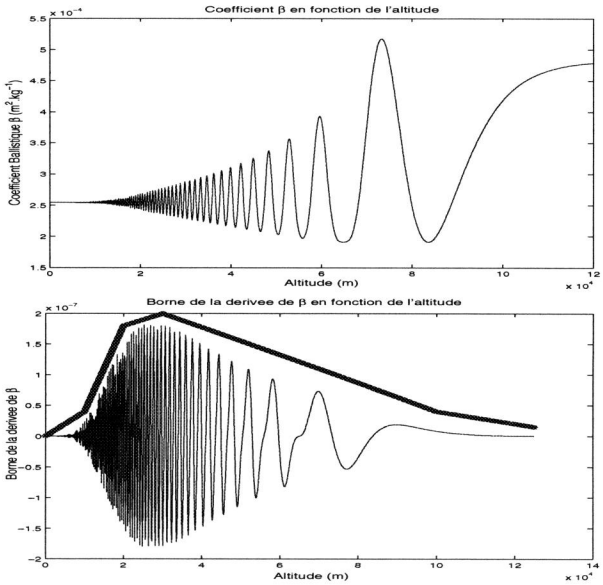

Figure 3: the coefficient β versus altitude and its derivative

On figure 3, we show on the left the derivative $\frac{d\beta}{dr}$ computed with the ballistic coefficient model we have used.
One should notice that we took a big enough envelope, then overestimated the dynamic noise. This will imply an over-evaluation of the PCRB during the simulations. In order to solve the problem, we will show in the simulations the evaluation of the PCRB with the exact envelope of the oscillations.

Comparison between particle filter and EKF, Robustness
We present the results obtained with a well known dynamic noise on figure 4. If the dynamic noise is under-evaluated, we obtain the figure 5.
Interpretation of the results

a) Perfectly evaluated dynamic noise.
On figure 4, we show the comparisons between particle and EKF filter, RMS error and PCRB.
The dynamic noise for the black, blue and red graphs is the dynamic noise given by the large envelope of figure 3.
The dynamic noise for the green graph is the exact envelope of the graph of figure 3.
The best estimation of the bound is done when the dynamic noise is evaluated with the exact envelope.
The behaviour of the EKF is exactly the same as the case of a set β, the EKF remains stuck on the initial value until the gain becomes big enough. This explains why the EKF error is getting through PCRB in the first part of the trajectory. More precisely, let us refer to figure 3. The first estimate of β is the value

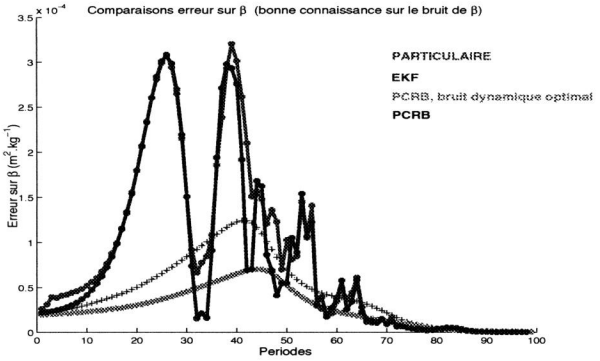

Figure 4: Error on the coefficient β

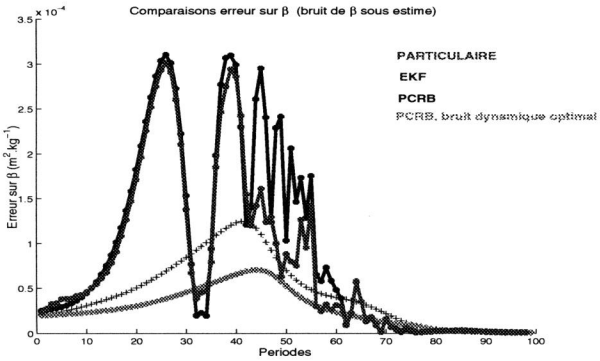

Figure 5: Error on the coefficient β

on the very right on the graph, added to a noise. This particular evolution of the coefficient produces the following event: if the estimate remains blocked, the error increases and then becomes exactly the same as the beginning around the altitude of 75 km.
On figure 4, the PCRB graphs obtained with large and exact envelopes are the same.
Eventually, we may say that when the dynamic noise is well evaluated, the particle and EKF filters are equivalent.

b) Under-evaluated dynamic noise.
By under-evaluated dynamic noise, we mean a dynamic noise on β equal to the dynamic noise given by the large envelope of the β oscillations, divided by ten. Given the simulation results of figure 4, it is clear that the particle filter's robustness is higher than the EKF's. When the dynamic noise is not well evaluated, Kalman gains are very far from the optimal gains. The particle filter estimates the value of β earlier than EKF.

4 Conclusion

The FIM, the CRB inverse, says that in the observability is proportional to the object's acceleration. Using the Allen solution, we gave an analytical approximation of the CRB of the ballistic coefficient β. This analytical function gives a two-step evolution and thus a two-step observability, these steps are related to the dynamical pressure brutal evolution versus time .

The PCRB shows that the ballistic coefficient is not immediatly observable. The evolution of the estimation error unfolds in two steps. First, periods where the re-entry is not really started, and where the error is increasing. Second, the RV reaches dense atmospheric layer, leading to a fast decrease of the error. This decrease was announced by the analytic FIM study.

During the comparison study between PCRB and tracking algorithm, it appeared that the knowledge of the variations of β is fundamental to obtain the correct dynamic noise dimension. This knowledge is ideal if we know the object, its initial incidence angle and the drag dependancy on the initial angle. If this knowledge is imperfect, the particle filter gives a better robustness than the EKF. If the knowledge is perfect, the EKF has excellent performance. The PCRB shows precisely the instants of the estimation algorithm optimality, and the instants of possible improvement.

Lemma 1 *The approximations given in equations (11,12,13,14,15) are valid.*

a) Equations (11) and (12)
Let us recall the dynamical system:

$$v[y(t)] = v(t_0)exp(-\frac{1}{2sin(\gamma)}\beta\rho_0 c_\rho e^{-\frac{y(t)}{c_\rho}}). \quad (22)$$

$$y(t) = sin(\theta_0)r(t_0) - \int_{t_0}^{t} v[y(\tau)]sin(\gamma)d\tau \quad (23)$$

Let us differentiate equation (22), we obtain

$$\frac{\partial v[y(t)]}{\partial r(t_0)} = \frac{\rho(t)\beta v[y(t)]}{2sin(\gamma)}\frac{\partial y(t)}{\partial r(t_0)} = \frac{\epsilon(t)}{sin(\gamma)}\frac{\partial y(t)}{\partial r(t_0)} \quad (24)$$

$$\frac{\partial v[y(t)]}{\partial v[y(t_0)]} = \frac{\rho(t)\beta v[y(t)]}{2sin(\gamma)}\frac{\partial y(t)}{\partial v[y(t_0)]} + \frac{v[y(t)]}{v[y(t_0)]} = \frac{\epsilon(t)}{sin(\gamma)}\frac{\partial y(t)}{\partial v[y(t_0)]} + \frac{v[y(t)]}{v[y(t_0)]} \quad (25)$$

If we differentiate equations (23), we obtain

$$\frac{\partial y(t)}{\partial r(t_0)} = sin(\theta_0) - \int_{t_0}^{t}\frac{\partial v(\tau)}{\partial r(t_0)}sin(\gamma)d\tau \quad (26)$$

$$\frac{\partial y(t)}{\partial v[y(t_0)]} = -\int_{t_0}^{t}\frac{\partial v(\tau)}{\partial v[y(t_0)]}sin(\gamma)d\tau \quad (27)$$

If we substitute equation (26) in (24) and equation (27) in (25), we obtain:

$$\frac{\partial v[y(t)]}{\partial r(t_0)} = \frac{\epsilon(t)}{sin(\gamma)}sin(\theta_0) - \frac{\epsilon(t)}{sin(\gamma)}\int_{t_0}^{t}\frac{\partial v[y(\tau)]}{\partial r(t_0)}sin(\gamma)d\tau$$

$$\frac{\partial v[y(t)]}{\partial v[y(t_0)]} = -\frac{\epsilon(t)}{sin(\gamma)}\int_{t_0}^{t}\frac{\partial v[y(\tau)]}{\partial v[y(t_0)]}sin(\gamma)d\tau + \frac{v[y(t)]}{v[y(t_0)]}$$

or, by setting $S = \int_{t_0}^{t}\frac{\partial v[y(\tau)]}{\partial r(t_0)}d\tau$ and $T = \int_{t_0}^{t}\frac{\partial v[y(\tau)]}{\partial v[y(t_0)]}d\tau$:

$$S' = \frac{\epsilon(t)}{sin(\gamma)}sin(\theta_0) - \epsilon(t)S \quad (28)$$

$$T' = -\epsilon(t)T + \frac{v[y(t)]}{v[y(t_0)]}. \quad (29)$$

$$S(0) = 0, T(0) = 0 \quad (30)$$

This can be solved to give (just differentiate to verify):

$$S = e^{-\int_{t_0}^{t}\epsilon(s)ds}\int_{t_0}^{t} e^{\int_{t_0}^{s}\epsilon(w)dw}\frac{\epsilon(s)}{sin(\gamma)}sin(\theta_0)ds \quad (31)$$

$$T = e^{-\int_{t_0}^{t}\epsilon(s)ds}\int_{t_0}^{t} e^{\int_{t_0}^{s}\epsilon(w)dw}\frac{v[y(s)]}{v[y(t_0)]}ds. \quad (32)$$

Now we substitute equation (31) and (32) in (28) and (29):

$$|\frac{\partial v[y(t)]}{\partial r(t_0)}| = |S'| \leq \frac{\epsilon(t)sin(\theta_0)}{sin(\gamma)} + \epsilon(t)\int_{t_0}^{t}\frac{\epsilon(s)sin(\theta_0)}{sin(\gamma)}ds$$

$$|\frac{\partial v[y(t)]}{\partial v[y(t_0)]}| = |T'| \leq \frac{v[y(t)]}{v[y(t_0)]} + \epsilon(t)\int_{t_0}^{t}\frac{v[y(s)]}{v[y(t_0)]}ds$$

This proves formula (11) and (12).

b) Equations (13) and (14)
To prove formula (13), and (14), one should notice that $\dot{v} = \frac{1}{2}\rho(t)\beta v^2$ and then

$$\frac{d}{dt}\frac{\partial v[y(t)]}{\partial r(t_0)} = \frac{\partial \dot{v}[y(t)]}{\partial r(t_0)} = 2\epsilon(t)\frac{\partial v[y(t)]}{\partial r(t_0)}$$

$$\frac{d}{dt}\frac{\partial v[y(t)]}{\partial v[y(t_0)]} = \frac{\partial \dot{v}[y(t)]}{\partial v[y(t_0)]} = 2\epsilon(t)\frac{\partial v[y(t)]}{\partial v[y(t_0)]}$$

and the approximations of equations (11) and (12) give the result.

c) Equation (15)
Using equation (22), one can obtain:

$$\frac{\partial v}{\partial \beta} = v(-\frac{1}{2sin\gamma}\rho c_\rho)$$

hence

$$\frac{d}{dt}\frac{\partial v}{\partial \beta} = \frac{\partial}{\partial \beta}\frac{1}{2}\beta\rho v^2 = \frac{1}{2}\rho v^2 \times (1 - 2\epsilon\frac{\rho c_\rho}{vsin(\gamma)})$$

But c_ρ and v are of the same order. $c_\rho = 7000$ and $v = c \times 1000m.s^{-1}$. This proves the formula (15)

Lemma 2 *Let p be a real parameter, like $r(t_0)$,$v[y(t_0)]$ or β.*
Let $r = X + \frac{1}{2}\frac{Y^2}{X}$
such as $X = r(t_0) + \int_{t_0}^{t} v_r d\tau, Y = \int_{t_0}^{t} v_a d\tau$. then

$$\frac{\partial r}{\partial p} = \frac{\partial X}{\partial p} + \frac{\partial Y}{\partial p}\frac{Y}{X} - \frac{1}{2}(\frac{Y}{X})^2\frac{\partial X}{\partial p} \quad (33)$$

and

$$\frac{d}{dt}\frac{\partial r}{\partial p} = \frac{\partial v_r}{\partial p} + \frac{\partial Y}{\partial p}\frac{d(\frac{Y}{X})}{dt} + \frac{Y}{X}\frac{\partial v_a}{\partial p} - \frac{1}{2}\frac{\partial v_r}{\partial p}(\frac{Y}{X})^2 - \frac{Y}{X}\frac{d(\frac{Y}{X})}{dt}\frac{\partial X}{\partial p}$$

if $X >> Y$ then

$$\frac{d}{dt}\frac{\partial r}{\partial p} \approx \frac{\partial v_r}{\partial p} + \frac{\partial Y}{\partial p}\frac{v_a}{X} + \frac{Y}{X}\frac{\partial v_a}{\partial p} - \frac{1}{2}\frac{\partial v_r}{\partial p}(\frac{Y}{X})^2 \quad (34)$$

and

$$\frac{d^2}{dt^2}\frac{\partial r}{\partial p} \approx \frac{\partial \dot{v}_r}{\partial p} + \frac{\partial v_a}{\partial p}\frac{v_a}{X} + \frac{\partial Y}{\partial p}\frac{\dot{v}_a}{X} + \frac{v_a}{X}\frac{\partial v_a}{\partial p} + \frac{Y}{X}\frac{\partial \dot{v}_a}{\partial p} \quad (35)$$

Proof: For the first part, it is a simple application of differential calculus. For the second part, we just have to remark that:

$$\frac{d(\frac{Y}{X^2})}{dt} = \frac{v_a}{X^2} - 2v_r\frac{Y}{X^3} \approx 0 \qquad \frac{d(\frac{Y}{X})}{dt} = \frac{v_a}{X} - Y\frac{v_r}{X^2} \approx \frac{v_a}{X}$$

$$\frac{1}{X}\frac{d(\frac{Y}{X})}{dt} = \frac{v_a}{X^2} - Y\frac{v_r}{X^3} \approx 0 \qquad \frac{d(\frac{1}{X})}{dt} = -\frac{v_r}{X^2} \approx 0$$

References

[1] G.P. Cardillo, A. V. Mrstick and T. Plambeck *A Track Filter for reentry Objects with Uncertain drag* IEEE Transactions on Aerospace and Electronic systems, Vol 35, n2, April, 1999

[2] P.J. Costa and W.H. Moore, *Extended Kalman-Bucy Filters for Radar tracking and Identification* Proceedings of the 1991 IEEE National radar conference, IEEE Aerospace and Electronic Systems Society, 1991, pp. 127-131

[3] Pierre Minvielle *Tracking a ballistic Re-entry Vehicle with a Sequential Monte-Carlo Filter* 2002 IEEE Aerospace conference March 9-16 , 2002.

[4] Petr Tichavsky, Carlos H. Muravchink, Aye Nehorai *Posterior Cramer-Rao Bounds for Disrete-Time Nonlinear filtering* IEEE Transaction on signal processing vol 46, no 5 may 1998

[5] A. Farina, B.Ristic, D. Benvenuti *Tracking a Ballistic Target, comparison of Several nonlinear Filters* IEEE Trans. on aerospace and electronic systems July 2002 Vol 38 number 3.

[6] H. Jullian Allen, Murray Tobak *Dynamic stability of vehicles ascending or descending paths through the atmosphere* NACA Technical note 4275 july 1958

[7] B. Ristic, S. Arulampalam, J. Mc Carthy *Target Motion Analysis Using Range-only Measurements: Algorithms, Performance and Application to INGARA ISAR Data* DSTO-TR-1095, January 2001

[8] H. Jullian Allen, *Motion of a ballistic missile angularly misaligned with the flight path upon entering the atmosphere and its effect upon aerodynamic heating, aerodynamic loads, and miss distance* NACA Technical note 4048 october 1957

[9] H. Jullian Allen, A.J. Eggers, Jr. *A study of the motion and aerodynamic heating of ballistic missiles entering the earth's atmosphere at high supersonic speeds* NACA Technical note 1381

[10] Jean-Pierre Lecadre, *Properties of estimability criteria for target motion analysis*, IEE proceedings in Radar, Sonar Navigation No 2, April 1998